



---

**Visualization Methods for Loop Mediated Isothermal Amplification (LAMP) Assays.**

Journal:	<i>Analyst</i>
Manuscript ID	AN-MRV-10-2024-001287.R2
Article Type:	Minireview
Date Submitted by the Author:	20-Jan-2025
Complete List of Authors:	Novi , Vinni ; Regents of the University of Minnesota, Bioproducts and Biosystems Engineering Meher, Anil Kumar; University of Minnesota College of Food Agricultural and Natural Resource Sciences, Bioproducts and Biosystems Engineering Abbas, Abdenour; University of Minnesota, Department of Bioproducts and Biosystems Engineering

## Visualization Methods for Loop Mediated Isothermal Amplification (LAMP) Assays.

Vinni Thekkudan Novi<sup>1</sup>, Anil Kumar Meher<sup>1</sup> and Abdennour Abbas<sup>1</sup>

<sup>1</sup>Department of Bioproducts and Biosystems Engineering, University of Minnesota, St. Paul, MN 55108, U.S.A.

Corresponding author: A. Abbas; E-mail: aabbas@umn.edu

### Abstract

Recent advances in nucleic acid (NA) detection techniques have significantly enhanced the diagnosis of diseases caused by a range of pathogens. These NA-based methods that target specific gene sequences for identification offer high specificity. Despite the effectiveness of polymerase chain reaction (PCR), its requirement for sophisticated laboratory settings and expensive equipment restricts its accessibility, particularly in resource-limited settings. As an alternative, isothermal nucleic acid amplification methods are highly sought after due to their rapid, sensitive, and specific detection ability. Among these, loop mediated isothermal amplification (LAMP) stands out due to its simplicity, reliability, and cost-effectiveness. LAMP operates without the need for varied temperature cycles, employing a simple heating block to maintain a constant temperature, thus facilitating onsite rapid testing. In LAMP, the detection step is critical as it shows the outcome of the assay. In order to make the LAMP technique user-friendly and applicable for large scale testing, it is critical to have visual detection where the results can be observed with the naked eye. This review focuses on recent developments of LAMP visualization techniques, including the more common fluorescence, turbidity, and gel electrophoresis methods, as well as innovations in colorimetric techniques applying novel transduction methods such as nanoparticles and digital tools. Additionally, various practical applications of LAMP are discussed.

## 1. Introduction

Several nucleic acid (NA) detection techniques have been developed for the diagnosis of diseases caused by a wide range of pathogens including viruses, bacteria, and fungi. The NA-based detection method has been considered a highly accurate form of diagnosis since it targets specific gene sequences on the microorganism for identification. Although PCR is one among these, it can only be done in a laboratory setting due to the need to use equipment that requires multiple cycles of temperature variations. Not only does this make them expensive but also less accessible in resource-limited countries along with necessitating trained personnel. This may not fit all types of microbial detection requirements and so, alternative methods have been studied that can cut down the costs while still maintaining the same or higher sensitivity.<sup>1</sup>

Isothermal nucleic acid amplification methods have been explored as an alternative to PCR. These methods eliminate the need to use expensive thermocycling equipment for nucleic acid amplification since they do not require the maintenance of varying temperatures for each replication cycle. Further, the simplicity of the method gives flexibility to conduct the tests anywhere and by anyone, which is significant in reducing the cost and time taken. Some such methods include nucleic acid sequence-based amplification (NASBA), primer-generation rolling circle amplification (PG-RCA), strand displacement amplification (SDA), helicase-dependent amplification (HDA), and recombinase polymerase amplification (RPA).<sup>2, 3</sup> Among these NASBA, SDA, HDA and RPA require multiple enzymes to function. This greatly increases the complexity in optimizing the assay for various pathogen detection along with increasing the cost of reagents. RCA is specifically applied to copying target DNA of circular nature, which does not cover most of the pathogens generally tested.

1  
2  
3           Loop mediated isothermal amplification (LAMP) as the name suggests, is one other  
4 method that comes under this category. It is most popularly used for the development of rapid  
5 onsite tests due to its simplicity, reliability, and flexibility in optimizing reaction conditions  
6 and detection.<sup>4</sup> Similar to PCR this can be divided into two parts – a nucleic acid amplification  
7 step and a detection step. The reaction mixture uses four to six primers for target sequence  
8 amplification that makes it highly sensitive, and *Bst* polymerase enzyme that enables strand  
9 displacement in constant temperature.<sup>1</sup> This allows the reaction to be carried out using a  
10 simple heating block that can maintain a constant temperature between 60-65° C, which cuts  
11 down the cost and time taken to conduct the test.  
12  
13  
14  
15  
16  
17  
18  
19  
20  
21  
22  
23

24           An illustration of a typical LAMP mechanism is provided in **Figure 1**. The reaction  
25 begins when the polymerase enzyme displaces the double stranded target DNA at a constant  
26 temperature. This causes the primers to specifically hybridize with six to eight regions of the  
27 target DNA, leading to the amplification process. Two of the primers form a loop structure,  
28 which further facilitates multiple rounds of amplification and generate several nucleic acid  
29 strands of various sizes. In addition to the new amplicons, byproducts such as pyrophosphate  
30 ions and protons get accumulated in the reaction mixture. These have been used as indicators  
31 of a LAMP reaction based on which several visualization methods have been formulated.<sup>5</sup>  
32  
33 While the most common/standard methods of LAMP detection include fluorescence, turbidity,  
34 and gel electrophoresis, other detection techniques developed based on colorimetric principles  
35 include the use of dyes and nanoparticles. Tools such as smartphone applications,<sup>6</sup> multiplex  
36 assays, microfluidic devices,<sup>7</sup> etc. were also developed to aid in the visualization process using  
37 the above mechanisms. Therefore, this review is focused on discussing the current LAMP  
38 reporting techniques, critically analyzing their limitations and possibilities for improvement.  
39  
40  
41  
42  
43  
44  
45  
46  
47  
48  
49  
50  
51  
52  
53  
54  
55  
56  
57  
58  
59  
60

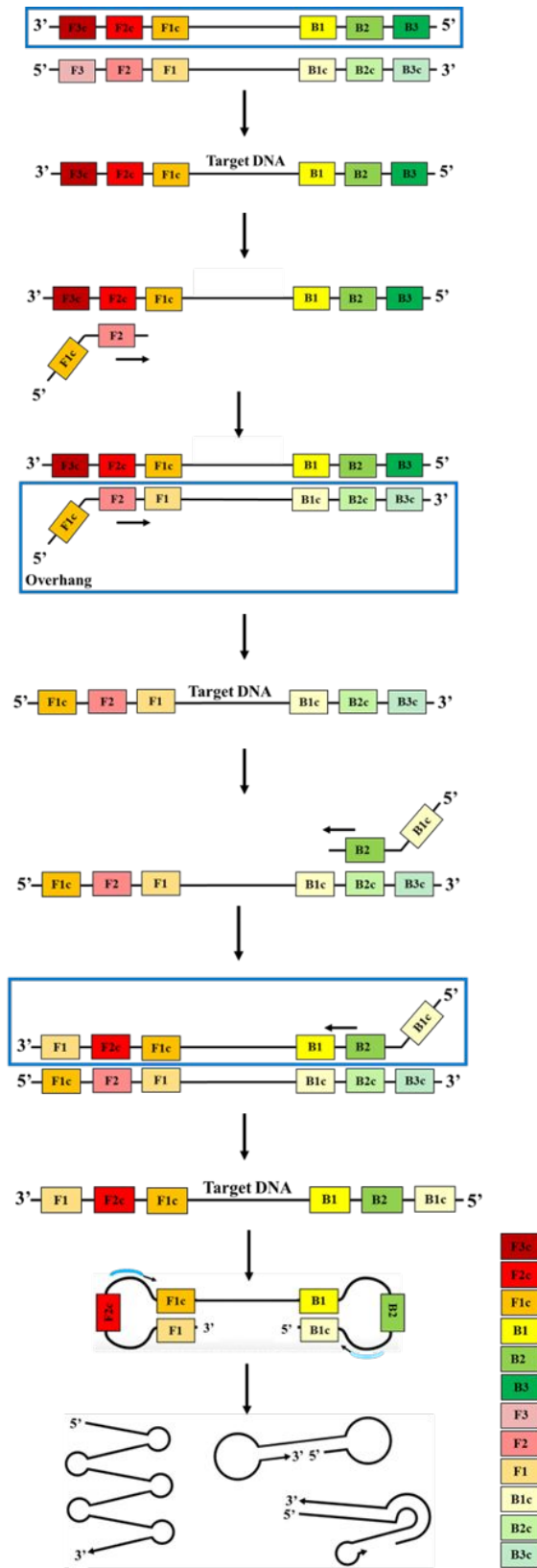
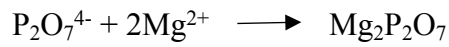
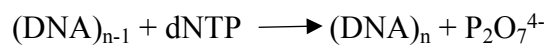


Figure 1. LAMP reaction steps.

## 2. Turbidity-based LAMP detection

Turbidity after a LAMP reaction occurs due to the precipitation of magnesium pyrophosphate which is a byproduct of nucleic acid replication. New DNA/RNA strand synthesis is accompanied by the formation of negatively charged phosphates which binds to the divalent magnesium cations from the salts in the buffer. Therefore, measuring this turbidity directly correlates to the number of amplicons formed during the reaction.<sup>8</sup>



Usually, turbidity could be seen using the naked eye. However, people with poor eyesight may have difficulty with distinguishing positive and negative samples. It must also be noted that the sample size for LAMP reactions is usually around 25  $\mu\text{l}$ ,<sup>9, 10</sup> which is too small for such accurate distinctions. For this purpose, conventionally, turbidity from a LAMP reaction product is measured using a turbidimeter and compared for confirmation.

Some studies have included advancements to the turbidity-based LAMP detection for fast and reliable results.<sup>11-13</sup> One of the studies used a real-time turbidimeter to monitor turbidity in LAMP reactions containing single, duplex and triple templates for chicken parvovirus, chicken infectious anaemia virus, and fowl aviadenovirus serotype 4. The turbidity signal came out the fastest when multiple reactions were conducted. This shows that the real time turbidity measurement system can be used for monitoring multiple reactions simultaneously. However, it could not identify the pathogen template that caused the positive result, which may be necessary to diagnose diseases.<sup>12</sup>

1  
2  
3 The advantage of using turbidity as an indicator is that it does not require opening the  
4 reaction tubes for post processing to enable detection of DNA. This reduces the possibility of  
5 cross contaminations while processing multiple samples over time. However, the turbidity -based  
6 LAMP detection presents challenges in real-world applications. The reliance on turbidimeters,  
7 which are not portable, increases cost and limits usability in resource-limited environments.  
8 Additionally, samples with high protein content, such as blood or tissue lysates, exacerbate the  
9 issue of false positives due to non-specific turbidity from protein precipitation.<sup>14</sup> Furthermore,  
10 the transient nature of turbidity signals, which quickly diminish, poses a risk for false negatives  
11 if measurements are delayed. Magnesium pyrophosphate, the byproduct responsible for turbidity,  
12 precipitates temporarily and begins to dissolve or settle over time. If measurements are not  
13 performed immediately after the reaction, the turbidity can diminish, leading to false negatives or  
14 inconsistent readings, particularly in high-throughput settings.<sup>14, 15</sup> While real-time turbidimeters  
15 can monitor multiple reactions simultaneously, they are incapable of distinguishing between  
16 different target templates in multiplex assays. This inability to identify the specific pathogen or  
17 target amplicon further restricts its diagnostic utility in cases where multi-pathogen detection is  
18 essential. Studies by Francois and co-workers have demonstrated that turbidity-based LAMP  
19 assays could detect *Salmonella enterica* serovar Typhi DNA with a sensitivity of 500  
20 femtograms, approximately eight genome copies, highlighting their comparable performance to  
21 optimized qPCR assays.<sup>14</sup> However, the detection efficiency diminishes at DNA concentrations  
22 below this threshold, and challenges such as false-positive signals in whole blood samples  
23 underscore the need for optimized protocols in complex matrices.  
24  
25  
26  
27  
28  
29  
30  
31  
32  
33  
34  
35  
36  
37  
38  
39  
40  
41  
42  
43  
44  
45  
46  
47  
48  
49  
50  
51  
52  
53  
54  
55  
56  
57  
58  
59  
60

### 3. Fluorescence-based LAMP detection

Fluorescent resonant energy transfer (FRET)-based detection of LAMP products generally relies on the use of fluorescent dyes, probes, or nanoparticles as signal transducers to detect amplicons. As nucleic acid amplification occurs, the intensity of fluorescence from LAMP products increases, which is measured at the end of the reaction using an appropriate fluorescence device. This type of detection also allows real time monitoring of the fluorescence similar to the turbidity measurement.<sup>1</sup> In laboratory settings, the fluorescence can be measured using a spectrofluorometer, which has a broad range of excitation and emission wavelengths that make it flexible for applications with most fluorescent agents used in LAMP. It is also proven to be highly specific and sensitive.

#### 3.1. Fluorescent dyes

Ethidium bromide, SYBR Green I and EvaGreen are some common dyes used to generate fluorescence signals in LAMP reactions. Their fluorescence mechanism is based on their ability to intercalate within double-stranded DNA (dsDNA) structures that usually get generated in the form of amplicons in LAMP.<sup>16, 17</sup> Since ethidium bromide is more carcinogenic in nature, most LAMP-based fluorescence detection methods have used SYBR Green I dye. However, one of its major drawbacks is its non-specific interaction with any dsDNA. This means that this method not only measures fluorescence from dye bound to specific amplicons generated in the LAMP but also to background and non-specifically formed dsDNA. This creates problems in getting accurate results. It must also be noted that the real-time fluorescence curves obtained in LAMP assays using intercalating dyes may deviate from the typical sigmoidal pattern seen in PCR, often resembling a 'hat-shaped' curve. This apparent decline in fluorescence intensity at later stages of the reaction is not due to a reduction in the actual fluorescence signal but results



1  
2  
3 from optical interference caused by the precipitation of magnesium pyrophosphate, as described  
4 by Peyrefitte and co-workers.<sup>18</sup> This phenomenon can be more profound towards the end of the  
5 reaction and may be significant when considering accurate data collection. Proper optimization  
6 and dye selection can mitigate these issues, ensuring accurate fluorescence detection.  
7  
8  
9

10  
11  
12  
13 Li and co-workers explored the possibility of combining two different dyes –  
14 hydroxynaphthol blue (HNB) and SYTO 9 in certain proportions to act as indicators of the  
15 amplification process. The SYTO 9 was chosen for its ability to intercalate between dsDNA  
16 similar to SYBR Green and HNB for its ability to chelate  $Mg^{2+}$  ions required for DNA  
17 replication. In this case, the dyes were added before the reaction began, at which point the  
18 samples emitted light green fluorescence. This is due to the intercalation of SYTO 9 dye with  
19 background dsDNA before the reaction began. Once the reaction was complete, the positive  
20 samples emitted brighter green fluorescence at 610 nm due to the increasing accumulation of  
21 SYTO 9 on the generated dsDNA target amplicons. During this time the  $Mg^{2+}$  ions bound to the  
22 pyrophosphate ions generated in the replication process and were absent for HNB binding.  
23  
24 However, the negative samples emitted red fluorescence at 505 nm due to the formation of the  
25 HNB- $Mg^{2+}$  complex. This is because of the absence of a target DNA strand that is required for  
26 DNA replication to occur, which leaves the  $Mg^{2+}$  ions free to bind to the HNB dye. Such distinct  
27 changes in fluorescence emission between the positive and negative samples solve issues  
28 associated with inaccurate reporting arising from wrong color perception. However, it still does  
29 not rule out the possibility of detecting a false positive sample as discussed earlier since the  
30 SYTO 9 dye does not differentiate between specific and non-specific dsDNA.<sup>19</sup>  
31  
32  
33  
34  
35  
36  
37  
38  
39  
40  
41  
42  
43  
44  
45  
46  
47  
48  
49  
50  
51

52  
53 Microfluidic platforms have garnered attention in the development of diagnostic systems  
54 and have not gone unnoticed for applications involving LAMP assays. Cao et al. demonstrated  
55  
56  
57  
58  
59  
60

1  
2  
3 the possibility of detecting multiple foodborne bacterial pathogens in milk using a microfluidic  
4 chip containing ten chambers. Each chamber is preloaded with specific primer sets  
5  
6 corresponding to a different pathogen along with positive and negative controls. The  
7  
8 microfluidic chip was designed to allow a single injection of the reaction mixture, including the  
9  
10 sample, into a distribution channel, after which the reaction was started. Although the reaction  
11  
12 takes 45 min, which is longer than most LAMP assays that take 30-35 min, the microfluidic  
13  
14 platform with the preloaded primers saves a lot more time in sample preparation. Both  
15  
16 fluorescence and visual detection options were explored for quantitative and qualitative analysis,  
17  
18 respectively. EvaGreen dye (another nucleic acid intercalating dye) served as an indicator for  
19  
20 fluorescence-based detection, which was measured at the end of the reaction using a LAMP  
21  
22 instrument. While this may not be ideal for field testing, the development of an appropriate  
23  
24 qualitative visualization for the microfluidic platform can prove to be effective for point-of-care  
25  
26 tests.<sup>2, 20</sup>  
27  
28  
29  
30  
31  
32  
33

### 34 **3.2. Fluorescent nanoparticles**

35  
36  
37 Semiconductor fluorescent nanoparticles such as quantum dots (QDs) have been studied  
38  
39 for their photostable property. Several LAMP studies have used QDs modified with proteins or  
40  
41 oligonucleotide/primer sequences to act as fluorescent labels for the generated amplicons.  
42  
43 However, most of these have multiple steps that increase the time to result or require post-  
44  
45 amplification open-tube procedures which increases the risk of carryover contamination.  
46  
47 Although some studies have focused on eliminating these problems, the preparation of the  
48  
49 modified QD probes is expensive. To overcome these issues, Lee *et al.* synthesized amine  
50  
51 functionalized QDs that can be added to the reaction mixture before amplification and are less  
52  
53 expensive due to the simplicity of the synthesis. Specifically, cysteamine-modified CdSeS/ZnS  
54  
55  
56  
57  
58  
59  
60

1  
2  
3 QDs were synthesized. Here, the negatively charged amine group acts as a link between the QDs  
4 and magnesium pyrophosphate crystals ( $\text{Mg}_2\text{P}_2\text{O}_7$ ) that are generated during nucleic acid  
5  
6 amplification in positive samples. This interaction causes the QDs to coprecipitate with the  
7  
8 crystals and settle to the bottom of the tube, which look like green, fluorescent precipitates under  
9  
10 fluorescence photography. In a negative sample, the  $\text{Mg}_2\text{P}_2\text{O}_7$  crystals are absent and so, the  
11  
12 negatively charged amine-QDs remain dispersed due to the interparticle electrostatic repulsion  
13  
14 and show uniform green fluorescence. This study shows the possibility of using both qualitative  
15  
16 and quantitative readout of the results.<sup>21</sup>  
17  
18  
19  
20  
21  
22  
23

24  
25 While fluorescence photography allows final qualitative confirmation, real time  
26  
27 fluorescence monitoring is highly efficient, sensitive, and specific and allows quantitative  
28  
29 analysis. However, given the need for a detection instrument for real time fluorescence  
30  
31 monitoring, this may not be suitable for field tests.<sup>22</sup>  
32  
33

34  
35 Although microfluidic platforms and portable fluorescence devices show promise for  
36  
37 multiplex detection and field deployment, these tools remain expensive, require specific  
38  
39 excitation and emission ranges, forcing the user to restrict their choice of dyes and add  
40  
41 complexity to the assay design.  
42  
43

#### 44 **4. Bioluminescence-based LAMP detection**

45  
46

47  
48 Like fluorescence, bioluminescence resonance transfer (BRET) has been applied to detect  
49  
50 LAMP amplicons in some studies. Although not as commonly used as fluorescence-based  
51  
52 detection, its mechanism remains similar, where, instead of an external light source that is used  
53  
54 to excite a fluorescent marker, light is produced when the enzyme luciferase oxidizes its  
55  
56  
57  
58  
59  
60

1  
2  
3 substrate luciferin. This excites the protein marker used to indicate the presence of dsDNA  
4  
5 generated using the LAMP assay. Since the light is produced inherently in BRET, this may  
6  
7 overcome some of the problems associated with FRET such as autofluorescence, light scattering,  
8  
9 or photobleaching.<sup>23</sup>  
10  
11

12  
13 Stigter and co-workers explored the application of BRET for LAMP amplicon detection  
14  
15 uses a luminescent multivalent intercalating dye (LUMID). Here, the intercalating dye used for  
16  
17 dsDNA detection is conjugated to a NanoLuc luciferase enzyme, which is blue light-emitting.  
18  
19 When the dye binds to dsDNA generated during a LAMP reaction, energy transfer from the  
20  
21 luciferase to the dye occurs, causing them to emit green luminescence (**Figure 2**). This change is  
22  
23 captured using a smartphone camera to record the results of the test. To improve the signal and  
24  
25 make the dsDNA binding stronger, the researchers combined multiple dyes with positively  
26  
27 charged lysine linkers and conjugated them closer to the active site of the luciferase enzyme.  
28  
29 This seems to be a requisite for better signal emissions and stronger binding of the dyes to the  
30  
31 dsDNA. However, apart from the advantage of not needing an external light source for the  
32  
33 detection of the LAMP amplicons,<sup>24</sup> the working of this visualization technique is the same as  
34  
35 using any intercalating fluorescent dye described in literature. The need to use multiple dye  
36  
37 components, the additional reagents, including the enzyme, and the varying conjugation routes,  
38  
39 seem to make the adoption of this potentially off-the-shelf visualization kit expensive.  
40  
41  
42  
43  
44  
45  
46  
47  
48  
49  
50  
51  
52  
53  
54  
55  
56  
57  
58  
59  
60

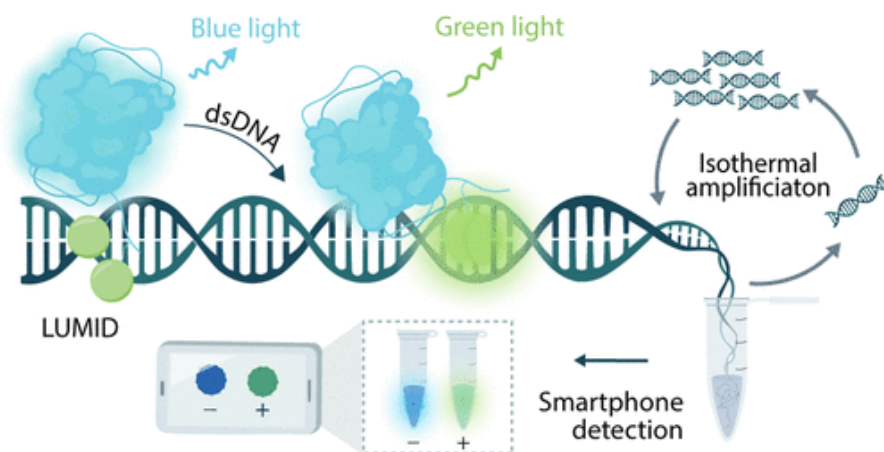


**Figure 2.** Schematic of the LUMID sensor.<sup>24</sup> Reprinted with permission from Ref. 22, Copyright (2022) American Chemical Society.

Other studies have combined real time LAMP (RT-LAMP) monitoring with bioluminescent assay in real time (BART) for the detection of various viral pathogens. A group of researchers studied the application of this RT-LAMP-BART system to detect different strains of SARS-CoV-2. The assay relies on the use of Lyophilized BART Master™ Reagent (Erba Mannheim, Ely, UK) which is added to the LAMP reaction mixture prior to amplification.<sup>14, 25</sup> In another study, hepatitis A virus was detected in inoculated food samples.<sup>25</sup> Given that the viral template is RNA, reverse transcription LAMP was performed, during which the generation of dsDNA caused precipitation of magnesium pyrophosphate in the reaction mixture. It is the formation of these inorganic pyrophosphates that is monitored using the bioluminescence signal.<sup>25-27</sup>

The mechanism of BART starts when the inorganic pyrophosphate is converted to adenosine triphosphate (ATP) by the enzyme ATP sulfurylase. Then the thermostable luciferase enzyme uses this ATP to oxidize the substrate luciferin and produce bioluminescence. A peak in the light signal is observed in positive samples when this phenomenon occurs, whereas the negative samples do not show any such peak. However, BART system still requires detection

1  
2  
3 devices to continuously keep track of these light signals from the LAMP reaction to identify that  
4 peak.<sup>28, 29</sup> The need for such an instrument could add to the cost of operation and the dependency  
5  
6 on a laboratory setup.<sup>22</sup>  
7  
8  
9

10 Bioluminescence-based detection, such as BRET and BART, addresses autofluorescence  
11 and photobleaching issues by relying on the intrinsic light produced during luciferase-mediated  
12 oxidation of luciferin. This enhances signal-to-noise ratios and sensitivity while allowing real-  
13 time monitoring. However, the need for additional reagents, enzyme conjugation, and specialized  
14 detection devices increases cost and complexity, limiting field applicability. Although  
15 smartphone-based imaging for bioluminescence signals shows potential, these systems often lack  
16 the precision required for diagnostics. Furthermore, bioluminescent methods relying on ATP  
17 production are susceptible to enzymatic inhibition, increasing the risk of false negatives.  
18  
19  
20  
21  
22  
23  
24  
25  
26  
27  
28  
29

30 Alternatively, colorimetric detection methods have been explored for LAMP  
31 visualization in field-based applications.  
32  
33  
34

## 35 **5. Colorimetric LAMP detection**

### 36 **5.1. Dye-based colorimetry**

#### 37 **5.1.1. Intercalating dyes**

38  
39  
40  
41 Generally, nucleic acid intercalating dyes used in LAMP assays tend to be fluorescent in  
42 nature and would require a fluorometer to detect the results. However, certain fluorescent dyes  
43 such as SYBR Green I, if used at a higher concentration, can indicate the presence or absence of  
44 a positive reaction through visual color change from orange to green. Some studies have  
45 explored this option to develop naked eye reporting of LAMP results. But the amplification  
46 process gets inhibited when the dye is used at such high concentrations. This makes it necessary  
47 to add the dye after the LAMP reaction unlike when it is used for fluorescence detection at low  
48  
49  
50  
51  
52  
53  
54  
55  
56  
57  
58  
59  
60

1  
2  
3 concentrations. They sometimes would also require a UV lamp for better visualization. The  
4 malarial parasite, *Plasmodium knowlesi*, and SARS-CoV-2 are examples of some pathogens  
5 detected using this SYBR Green I LAMP assay.<sup>17, 30</sup> Typically, SYBR Green I function as a  
6 DNA indicator due to the presence of positive charges that help with binding to the negatively  
7 charged dsDNA. This DNA-dye complex then absorbs blue light and emits green light, which is  
8 used as a signal for positive reactions.<sup>31</sup> Other fluorescent dyes that could be used as colorimetric  
9 indicators based on similar mechanism include Quant-iT PicoGreen, which could be expensive,  
10 and EvaGreen dye.<sup>15</sup>

11  
12 Certain triphenylmethane dyes such as crystal violet, methyl green, fuchsin, and malachite green  
13 also operate based on their affinity to specifically bind with the major grooves of dsDNA.<sup>32</sup>  
14 When crystal violet interacts with sulfite ions, they turn colorless due to the formation of leuco  
15 crystal violet (LCV). In the presence of dsDNA, the colorless LCV turns back to its colored form  
16 crystal violet upon its strong binding to the DNA amplicon.<sup>33</sup>

17  
18 Fuchsin is another intercalating dye, which works similarly. It is magenta in color and  
19 upon interaction with sulfite ions turns to its colorless leucofuchsin form due to the loss of its  
20 chromophoric structure. However, when the acid-hydrolyzed DNA binds to this dye, the sulfite  
21 gets removed and the dye returns to its chromophoric structure. During this interaction, the dye  
22 looks purple.<sup>34</sup> Among the above discussed intercalating dyes, the advantage of  
23 triphenylmethane dyes over fluorescent dyes is that they do not inhibit the amplification process.  
24 This makes them flexible enough to be added to the LAMP mixture prior to amplification,  
25 reducing additional post amplification steps. Therefore, simpler LAMP assay designs could be  
26 developed for various pathogen detection.

27  
28  
29  
30  
31  
32  
33  
34  
35  
36  
37  
38  
39  
40  
41  
42  
43  
44  
45  
46  
47  
48  
49  
50  
51  
52  
53  
54  
55  
56  
57  
58  
59  
60

1  
2  
3 Schiff's reagent is a dye formulation obtained by the combination of fuchsin and sodium  
4 bisulfite. Thai and Lee directly used this reagent for the detection of hair loss related single  
5 nucleotide polymorphism (SNP) to eliminate the additional step of adding sodium sulfite. The  
6 study also describes the use of a foldable hand-sized chamber to conduct the colorimetric LAMP  
7 assay, which was then analyzed using the ImageJ software.<sup>35</sup>  
8  
9  
10  
11  
12  
13

14  
15 Although the intercalating dyes described above directly detect the dsDNA through  
16 visible color change in theory, they do suffer from showing a clear distinction between positive  
17 and negative samples in practice. Given that the sample size for a LAMP assay could be as small  
18 as 20  $\mu$ L, not being able to discern the color change can lead to false positives or negatives.<sup>36</sup> To  
19 overcome these issues, some studies have considered using image analysis software to record the  
20 changes in those hues using Red-Green-Blue (RGB) and Commission Internationale de  
21 l'Eclairage (CIE) Lab color spaces models.<sup>32</sup> However, having this additional step requires a  
22 visualizing instrument, which goes against the concept of a rapid cost-effective visualization  
23 method. Another potential problem with the use of intercalating dyes is that they could be  
24 toxic/mutagenic in nature. This is because they operate through their affinity for nucleic acids.<sup>37</sup>  
25 Care must be taken in handling and disposing of these reagents. While not all intercalating dyes  
26 are considered dangerous, and there are indeed safer dyes commercially available, the user must  
27 be cautious before choosing the right one.  
28  
29  
30  
31  
32  
33  
34  
35  
36  
37  
38  
39  
40  
41  
42  
43  
44  
45

### 46 **5.1.2. pH-sensitive dyes**

47  
48

49 To overcome the issues posed by intercalating dyes, many studies have explored the use  
50 of pH-sensitive dyes for detecting positive samples in a LAMP assay.<sup>36, 38-41</sup> The mechanism of  
51 detection is based on pH changes induced by the amplification process, where the generation of  
52 dsDNA strands leads to a significant release of protons ( $H^+$  ions), causing the solution to turn  
53  
54  
55  
56  
57  
58  
59  
60



1  
2  
3 acidic. When the pH drops, the dye in the solution changes color.<sup>15</sup> This is usually a sharp  
4  
5 contrast that is easily discernible. Additionally, most pH-sensitive dyes do not inhibit LAMP and  
6  
7 can be added to the reaction mixture prior to amplification, making them more convenient to  
8  
9 employ. The following reaction sequences show the mechanism of pH-based dyes for the  
10  
11 detection of nucleic acids.<sup>42</sup>  
12  
13

14  
15 With Bst DNA polymerase:  $f\text{DNA} + \text{dNTPs} \rightarrow \text{DNA}^{+1} + \text{P}_2\text{O}_4^{-7} + \text{H}^+$   
16  
17

18 Hydrolysis reaction:  $\text{P}_2\text{O}_7^{4-} + \text{H}_2\text{O} \rightarrow 2\text{PO}_4^{3-} + 2\text{H}^+$   
19  
20

21 The most used pH sensitive dye is phenol red, which changes from dark pink to orangish  
22  
23 yellow color in a positive sample. Due to its distinct color change and ease of use, it has been  
24  
25 included in the commercial LAMP kits developed by New England Biolabs, a company that  
26  
27 specifically provides reagents and master mixes for LAMP assays. The WarmStart<sup>®</sup> Colorimetric  
28  
29 LAMP 2X Master Mix (DNA & RNA) consists of phenol red as the indicator dye and Bst  
30  
31 polymerase enzyme that only activates at temperatures above 60°C.<sup>43</sup> Several studies that used  
32  
33 phenol red as an indicator, have used this colorimetric master mix to conduct their LAMP assays.  
34  
35 At the end of the reaction, the results are recorded based on the color change observed in the  
36  
37 LAMP mixture.<sup>38, 44-50</sup>  
38  
39  
40  
41

42 Alternatives to phenol red were explored by a group of researchers to overcome the issue  
43  
44 of confusion in color perception by different individuals. This is because of the slow change  
45  
46 from red to yellow with phenol red could be shallow and ambiguous. For this purpose,  
47  
48 LAMPshade Magenta and LAMPshade Violet were used to develop a JaneliaLAMP (jLAMP)  
49  
50 for the detection of SARS-CoV-2 that showed steep and highly contrasting color changes. Apart  
51  
52 from naked eye detection, the color change can also be detected under UV lamp due to their  
53  
54  
55  
56  
57  
58  
59  
60

1  
2  
3 fluorescent nature. However, the availability of these dyes may not be widespread, which could  
4  
5 limit their application.<sup>51</sup>  
6

7  
8 Several studies have also explored the use of other pH-sensitive dyes to develop rapid LAMP  
9  
10 visualization assays for various pathogens. **Table 1** below summarizes recent research in this  
11  
12 area.  
13  
14

15  
16 **Table 1.** List of colorimetric LAMP assays using pH-sensitive dyes  
17

pH-sensitive dye	pH range for color change	Colorimetric indication for positive	Target detected	References
<b>Bromothymol blue</b>	8.8 to 6.8	Blue to yellow	<i>Toxoplasma gondii</i>	42
<b>Cresol red</b>	8.8 to 7.2	Purple/pink to yellow	Food allergens; Human Papilloma viruses (HPV)	40, 52
<b>Neutral red</b>	8 to 6.8	Light orange/yellow to pink	African swine fever virus (ASFV); Singapore grouper iridovirus (SGIV); Chicken	36, 53, 54
<b>Xylenol orange</b>	<6.7	Purple to yellow	<i>Phytophthora</i> Species	39, 55
<b>Phenolphthalein</b>	<8.5	Pink to colorless	Vancomycin-resistant <i>Enterococcus</i> (VRE)	41

18  
19  
20  
21  
22  
23  
24  
25  
26  
27  
28  
29  
30  
31  
32  
33  
34  
35 Apart from the straightforward LAMP reaction for the visual indication of amplification using  
36  
37 dyes, some studies<sup>59, 56</sup> have explored some innovative platforms to conduct the colorimetric  
38  
39 assay. Phenolphthalein-based test swabs were developed in another study as a post-reaction kit.  
40  
41 An osteoarthritis marker MTF1 gene was tested using LAMP, which was then evaluated using  
42  
43 the phenolphthalein swab. A change from pink to colorless on the swab indicated a positive  
44  
45 reaction.<sup>56</sup>  
46  
47  
48  
49

50  
51 Most pH-sensitive dyes show a color change involving a short range of colors such as  
52  
53 purple, blue, pink, and yellow. To expand the color spectrum for people affected by color  
54  
55 weakness, Wu and co-workers explored the possibility of combining two or more dyes for  
56  
57  
58  
59  
60

1  
2  
3 LAMP visualization.<sup>57</sup> This study combined pH-sensitive dyes with some pH insensitive dyes  
4 such as phenol red-azure II, and phenol red-methylene blue that change from blue purple to  
5 green, and bromothymol blue-cresol red, and bromothymol blue-phenol red that changes from  
6 green to yellow. Though this study aimed at expanding the color spectrum, the tested  
7 combinations were not enough to add to that range. Further, the combinations of dye would just  
8 increase the complexity and the price of the indicators used.<sup>57</sup>  
9  
10  
11  
12  
13  
14  
15  
16  
17

18 Raddatz and co-workers tested the combination of different pH-sensitive dyes for LAMP  
19 assay. This was done with the aim of reducing errors in sample addition by tracking it through  
20 the inclusion of dyes. Both the reaction mixture (16  $\mu$ L) and the sample solution (4 $\mu$ L) had  
21 different dyes added to them. The study tested eight different pH sensitive dyes, of which  
22 bromothymol blue for the reaction mixture and phenol red for the sample was found to show the  
23 best contrast at the end of the LAMP assay. However, it seems that varying volumes of the  
24 reagents may produce variations in the result and must be optimized each time before use. This  
25 complexity undermines the need to track the appropriate addition of LAMP reagents and sample  
26 solution.<sup>58</sup>  
27  
28  
29  
30  
31  
32  
33  
34  
35  
36  
37  
38

39 While pH sensitive dyes have some advantages, there are some major limitations to their  
40 application for accurate colorimetric analysis. The first problem is the indirect nature of  
41 detection, where changes in the pH could occur due to several factors. This increases the chances  
42 of false positives. Due to this, LAMP reaction with crude DNA extracts may not give desirable  
43 results since there could be interfering factors that alter the pH of the reaction.<sup>59</sup> Another  
44 significant problem is the slow color change of the dyes under high buffer conditions. This is  
45 because the change in pH is lowered under high buffered conditions. This necessitates the  
46 application of low buffer concentration for LAMP reaction.<sup>60</sup> Furthermore, the perception of  
47  
48  
49  
50  
51  
52  
53  
54  
55  
56  
57  
58  
59  
60

1  
2  
3 color change using the pH-sensitive dyes can vary between users causing variations in color  
4  
5 reporting.  
6  
7

### 8 **5.1.3. Metal-indicating dyes**

9

10  
11 The amplification of nucleic acids produces pyrophosphate ions that bind to magnesium  
12 ions ( $Mg^{2+}$ ) already present in the LAMP reaction buffer forming  $Mg_2P_2O_7$ . Certain dyes are also  
13  
14 capable of binding to these  $Mg^{2+}$  ions and depending on their availability, change color. This  
15  
16 behavior is used as an indication of amplification in each tested sample.  
17  
18  
19

20  
21 Calcein, which is also a fluorescent dye, has been used for the naked eye colorimetric  
22  
23 detection of LAMP due to their ability to bind to  $Mg^{2+}$  ions. The colorimetric mechanism of  
24  
25 calcein is usually combined with the addition of  $MnCl_2$ , at which point the dye appears orange  
26  
27 due to fluorescence quenching. When pyrophosphate ions are produced, the  $Mn^{2+}$  ions from  
28  
29  $MnCl_2$  replace the  $Mg^{2+}$  ions, letting the calcein dye turn yellow/green. Based on this process,  
30  
31 the negative samples remain orange whereas the positive samples turn yellow/green.<sup>61, 62</sup>  
32  
33 Although some research has used calcein as an indicator, there have also been reports of the  
34  
35 difficulty in distinguishing color change.<sup>63</sup> Another major problem is the need to use  $MnCl_2$ ,  
36  
37 which at certain concentrations inhibits polymerase activity.  
38  
39  
40  
41

42  
43 Hydroxynaphthol blue (HNB) is another metal binding dye that is commonly used for  
44  
45 LAMP detection. HNB binds to  $Mg^{2+}$  ions and turns violet in a negative sample. During  
46  
47 amplification in a positive sample, the generation of pyrophosphates takes away the  $Mg^{2+}$  ions  
48  
49 leading to the dye turning sky blue.<sup>61</sup> Although several studies have used HNB as an indicator  
50  
51 dye,<sup>64, 65</sup> some studies have tried to combine its application with other dyes for better contrast.  
52  
53  
54  
55  
56  
57  
58  
59  
60

1  
2  
3 This is because the change from violet to sky blue is sometimes subtle and not enough for  
4  
5 conclusive reporting of LAMP outcome.<sup>52</sup>  
6  
7

8 Other less commonly used metal-sensitive dye includes Eriochrome Black T (EBT),  
9  
10 which also changes color based on the presence or absence of  $Mg^{2+}$ .<sup>62</sup> Similar to the mechanism  
11  
12 of pH sensitive dyes, the metal indicating dyes change color due to an indirect phenomenon as a  
13  
14 result of DNA amplification. These dyes do not directly detect the generated nucleic acids, rather  
15  
16 indicate the presence or absence of free divalent cations in the buffer that interacts with the  
17  
18 byproducts of amplification. Due to this the same problems occurring with pH sensitive dyes  
19  
20 could potentially affect the results of the LAMP assay with these dyes. Recently colorimetric  
21  
22 LAMP methods have demonstrated remarkable sensitivity, achieving detection limits as low as 5  
23  
24 copies per reaction or 0.2 copies/ $\mu$ L. This high level of sensitivity is comparable to that of  
25  
26 advanced real-time PCR methods while maintaining compatibility with complex sample matrices  
27  
28 and providing results within 30 minutes.<sup>10</sup>  
29  
30  
31  
32  
33

## 34 **5.2. Nanoparticle-based colorimetry**

35  
36

37 Most colorimetric LAMP assays are based on metal nanoparticles, especially noble  
38  
39 metals such as gold (AuNPs) and silver (AgNPs). Among these the most popular choice is  
40  
41 AuNPs due to their simple and straightforward approach to color change. These nanoparticles  
42  
43 exhibit certain optical properties that are different from their bulk counterparts. Surface plasmon  
44  
45 resonance-based colorimetry is a phenomenon in which absorption of light in the visible range  
46  
47 gives the nanoparticles a certain color that changes with the size of the nanoparticles or with their  
48  
49 assembly. This property has been exploited in several diagnostic assays for the detection of  
50  
51 microorganisms or their genetic material.<sup>66</sup> Visual detection of LAMP assay is no exception to  
52  
53 this. A basic mechanism of visualization involves the use of the metal nanoparticles conjugated  
54  
55  
56  
57  
58  
59  
60

1  
2  
3 with target-specific oligonucleotide sequences that bind to the amplified DNA after a LAMP  
4 reaction. Depending on the conditions induced in this mixture, the nanoparticles tend to remain  
5 dispersed or aggregate, causing them to change color from red to purple in case of AuNPs and  
6 colorless to deep brown in AgNPs. This way both positive and negative samples are  
7 distinguished from each other.  
8  
9

10  
11 Sun et al. explained the use of AuNPs conjugated with target-specific oligonucleotides  
12 for the detection of the shrimp pathogen *Vibrio parahaemolyticus*. After the LAMP assay was  
13 conducted, the amplification products were incubated with the AuNP-oligonucleotides and a  
14 certain concentration of NaCl. In the case of positive samples, the generated dsDNA hybridized  
15 with the oligonucleotides on the AuNPs causing them to remain dispersed and red even with  
16 NaCl in solution. However, in negative samples, due to the absence of dsDNA, the free AuNP-  
17 oligonucleotides aggregated in the presence of the NaCl solution and turned purple. Based on  
18 this activity, the LAMP samples were distinguished as positive or negative.<sup>67</sup>  
19  
20  
21  
22  
23  
24  
25  
26  
27  
28  
29  
30  
31  
32  
33

34 Another study explained the use of silver nitrate and quercetin to produce AgNPs in the  
35 presence of LAMP amplicons. The mechanism of detection was based on the formation of a  
36 complex between the nitrogenous bases of LAMP amplicons and silver ions. When quercetin is  
37 introduced to this complex under basic conditions, it acts as a reducing agent leading to the  
38 formation of AgNPs. At this point the solution turns deep brown indicating a positive LAMP  
39 reaction. In negative samples, because of the absence of LAMP amplicons, the silver nitrate  
40 remains in solution and no color change is observed when quercetin is added. Based on this  
41 mechanism, a foldable microdevice was fabricated that contained a reaction and detection  
42 chamber. The LAMP assay was carried out in the reaction chamber followed by addition of  
43 silver nitrate. Then the device was folded so that the detection chamber containing quercetin  
44  
45  
46  
47  
48  
49  
50  
51  
52  
53  
54  
55  
56  
57  
58  
59  
60

would interact with the components in the reaction chamber causing a color change, if positive (Figure 3). The final color change was analyzed using the ImageJ software.<sup>68</sup>

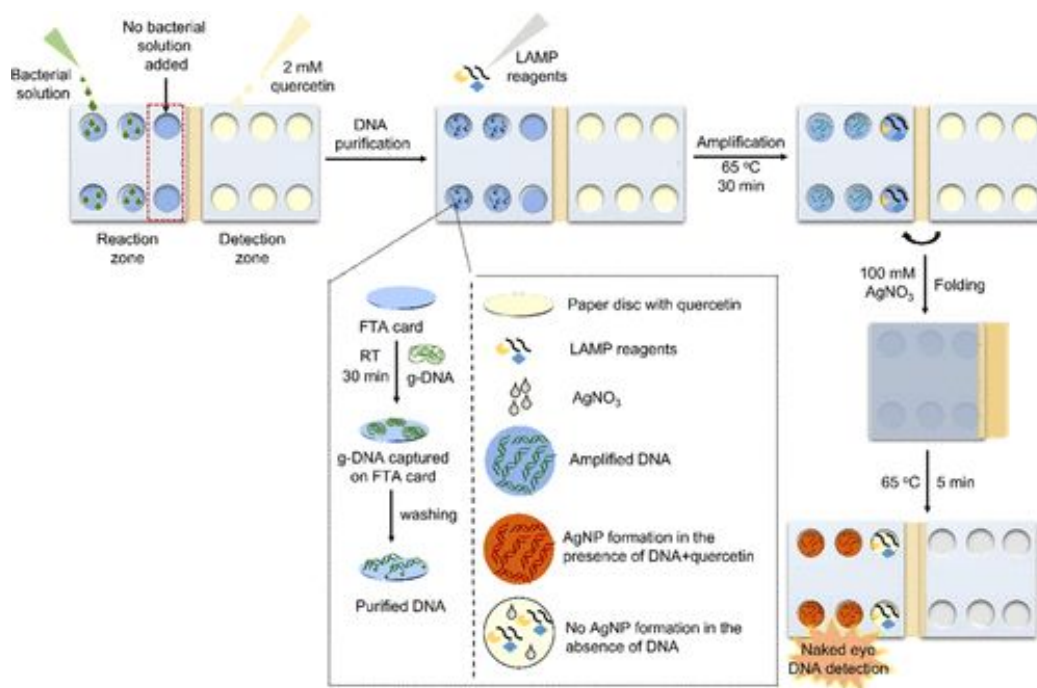


**Figure 3.** Design of the LAMP-AgNPs colorimetric assay using the foldable microdevice.<sup>68</sup> Reprinted with permission from Ref. 69, Copyright (2023) American Chemical Society.

In most such studies, the colorimetric detection of LAMP amplicons depended on the state of the nanoparticles – dispersed or aggregated. There are several factors that could induce aggregation of nanoparticles, leading to a color change. This may include varying buffer concentrations in the sample and other biological interferences. In some studies, changes in pH and/or ionic strength following amplicon generation lead to the aggregation of the AuNPs, resulting in a color change from red (single AuNPs) to purple (aggregated AuNPs) for detection.<sup>69-73</sup> However, this type of aggregation can occur due to other changes in the reaction medium that alters its pH or ionic strength irrespective of the presence or absence of amplified DNA. This could give rise to higher false negatives and decrease the sensitivity of the

1  
2  
3 assay.<sup>74</sup> Additionally, given that the sample size is small for most of these post-amplification  
4  
5 visualization tests, the changes observed in color most times are not as distinct, or may require  
6  
7 longer than the stipulated time to be visible. This causes the interpretation of results to be varied  
8  
9 among users.  
10

11  
12  
13 In summary, while colorimetric detection methods, including intercalating, pH-sensitive,  
14  
15 and metal-indicating dyes, provide accessible and low-cost solutions for LAMP visualization,  
16  
17 they are not without limitations. Issues such as inhibition of amplification, inconsistent color  
18  
19 changes, interference from crude samples, and reagent toxicity must be carefully addressed to  
20  
21 improve assay robustness. Future innovations could focus on developing safer, highly specific  
22  
23 dyes with enhanced visual contrast, as well as integrating automated image analysis tools to  
24  
25 minimize variability in result interpretation. These improvements will be essential to ensure  
26  
27 colorimetric LAMP methods achieve widespread adoption for rapid, point-of-care diagnostics.  
28  
29 Furthermore, optimizing reaction buffers to reduce background interference and designing robust  
30  
31 platforms, such as microfluidic devices or sealed reaction chambers, could enhance assay  
32  
33 performance in diverse sample matrices while reducing contamination risks. By overcoming  
34  
35 these technical barriers, colorimetric LAMP methods have the potential to transform diagnostics,  
36  
37 particularly in low-resource settings, where their affordability, simplicity, and portability make  
38  
39 them ideal for rapid, on-site nucleic acid detection.  
40  
41  
42  
43  
44  
45

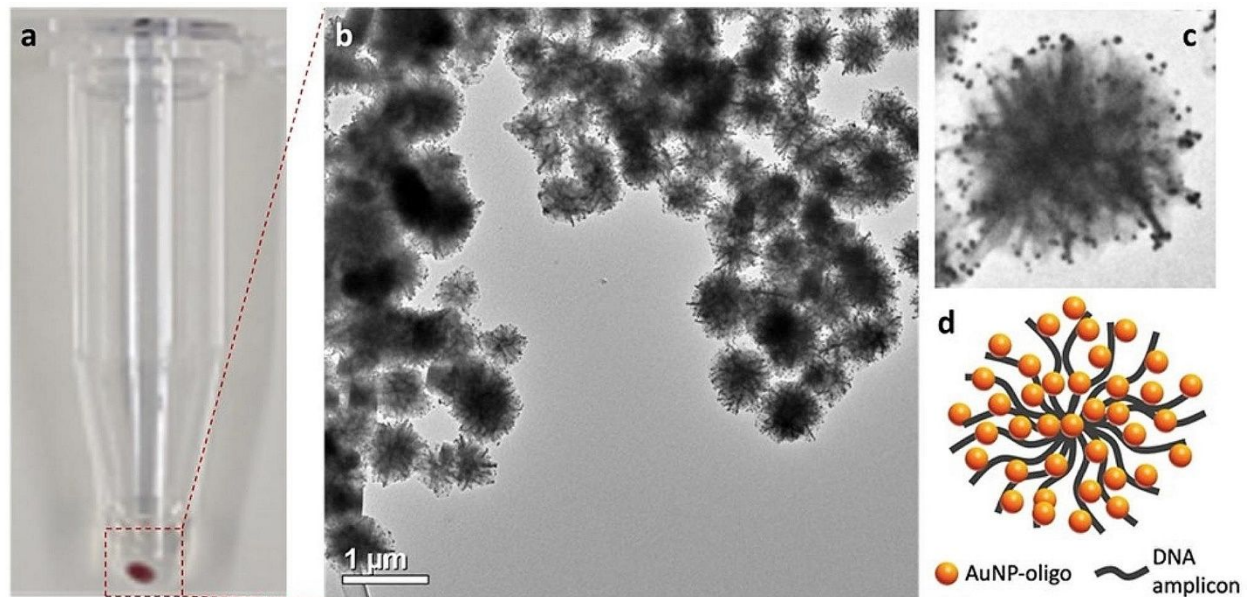
## 46 **6. Alternative LAMP Visualization**

47  
48

49 Visualization techniques in LAMP assays have significantly advanced with the  
50  
51 development of novel methods that make onsite nucleic acid detection more accessible and  
52  
53 reliable. As previously discussed, traditional colorimetric methods, while useful, often suffer  
54  
55 from limitations such as the need for precise dye concentrations. Furthermore, dye-based  
56  
57  
58  
59  
60



1  
2  
3 methods can be inhibited by the reagents in LAMP reactions, and subtle color shifts may not be  
4 consistently noticeable across different user groups, particularly for those with visual  
5 impairments. To address these challenges, a novel visualization method utilizing hierarchical  
6 nanoassembly of AuNPs was introduced. In this approach, oligonucleotide-conjugated AuNPs  
7 non-specifically bind to DNA amplicons produced in LAMP reactions, which upon inducing  
8 precipitation leads to the formation of distinct red pellets (**Figure 4**). This allows the amplicons  
9 to be detected as a colored pellet, visible to the naked eye, and eliminates the requirement of a  
10 specialized instrument for end point visualization. The absence of the amplicon also means the  
11 absence of the red pellet, which is clearly distinguishable even with varied eyesight. This method  
12 has shown significant improvements over traditional visualization techniques by offering higher  
13 sensitivity and faster detection times.<sup>75</sup>



53 **Figure 4.** Concept of amplicon visualization using hierarchical nanoparticle assembly. (a) The  
54 visible pellet at the bottom of the tube is formed following induced precipitation of assembled  
55  
56  
57  
58  
59  
60

1  
2  
3 AuNP-oligo with the DNA amplicons, (b) and (c) transmission microscope image of globular  
4 nanostructures, and (d) conceptual diagram of one assembled globule. The assembly of hundreds  
5 of these structures yields a red pellet visible to the naked eye.<sup>76</sup> Copyright © 2024, Vinni  
6  
7  
8  
9  
10 Thekkudan Novi et al.

11  
12  
13 The nanoassembly visualization technique was also demonstrated in a study where a  
14 LAMP assay was designed to detect *Bretziella fagacearum*, the pathogen responsible for oak  
15 wilt. The diagnostic system combines LAMP amplification with AuNP nanoassembly based  
16 visualization, allowing for naked-eye detection of the pathogen DNA when using both purified  
17 and crude DNA templates. This method has shown high diagnostic sensitivity and specificity,  
18 with the AuNPs acting as labels for the amplicons and a detection limit as low as  $1.87 \times 10^{11}$   
19 copies/mL.<sup>75, 76</sup> The advantage of this technique lies in its adaptability to field settings, as it does  
20 not require complex equipment, making it highly suitable for rapid diagnostics in remote  
21 locations. However, similar to some of the previously discussed detection systems, the post  
22 amplification step involving the AuNP nanoassembly requires opening the sample tube, which  
23 risks carryover contamination.<sup>76</sup> Additionally, the method's performance with crude biological  
24 samples, which may contain inhibitors, requires further evaluation to ensure robustness across  
25 diverse matrices. Future improvements, such as integration with microfluidic platforms, in-tube  
26 visualization designs,<sup>77, 78</sup> and automated image analysis tools, will enhance usability, minimize  
27 contamination risks, and enable reliable, onsite diagnostics for plant, animal, and human  
28  
29  
30  
31  
32  
33  
34  
35  
36  
37  
38  
39  
40  
41  
42  
43  
44  
45  
46  
47  
48  
49  
50  
51  
52  
53  
54  
55  
56  
57  
58  
59  
60

## 7. Conclusions

In conclusion, this review highlights the diverse visualization methods available for LAMP assays, each offering unique advantages and challenges that cater to specific diagnostic

1  
2  
3 needs. Fluorescence-based methods, using intercalating dyes, probes, or nanoparticles, enable  
4 highly sensitive and real-time monitoring of LAMP reactions, as do turbidity-based detection,  
5  
6 though their dependency on specialized instruments limits field applicability. Bioluminescence-  
7  
8 based detection eliminates the need for external light sources, offering sensitive detection  
9  
10 through luciferase-mediated light production, but requires additional reagents and equipment,  
11  
12 complicating its field deployment. Colorimetric detection, the most widely adopted method,  
13  
14 leverages pH-sensitive, intercalating, or metal-indicating dyes to produce visible color changes,  
15  
16 making it cost-effective and suitable for resource-limited or field-based settings. However,  
17  
18 challenges such as non-specific binding, subtle color transitions, and sample interference still  
19  
20 need to be addressed to further enhance its robustness. Nanoparticle-based approaches, such as  
21  
22 hierarchical nanoassembly of gold nanoparticles (AuNPs), provide robust, naked-eye detection  
23  
24 through visually distinct signals like red pellets, making them highly sensitive and adaptable for  
25  
26 field use. However, post-amplification handling increases the risk of contamination, which must  
27  
28 be mitigated through improved reaction tube designs or integrated workflows.  
29  
30  
31  
32  
33  
34  
35

36 Emerging technologies, including microfluidic platforms and hybrid detection systems,  
37  
38 integrate these visualization methods with portable and automated devices to streamline  
39  
40 workflows, enhance diagnostic accuracy, and reduce variability. Moving forward, innovations  
41  
42 aimed at improving signal specificity, minimizing contamination risks, and ensuring  
43  
44 compatibility with crude samples will be critical for advancing LAMP assays. By combining the  
45  
46 strengths of existing methods with commercial solutions and novel technologies, LAMP assays  
47  
48 have the potential to revolutionize diagnostic testing, delivering reliable, rapid, and accessible  
49  
50 tools for detecting plant, animal, and human pathogens in both laboratory and field settings.  
51  
52  
53  
54  
55  
56  
57  
58  
59  
60

**Author contributions:**

AA secured the funding, conceived the idea and provided technical direction and feedback. VTN and AM conducted the literature search for the review. VTN wrote the manuscript with input from all authors. AM organized the content and acquired permissions for figures.

**Conflicts of interest:**

The authors declare that they have no conflicts of interest.

**Funding:**

This work was supported by the Minnesota Environment and Natural Resource Trust Fund as recommended by the Legislative Citizen Commission on Minnesota's Resources, through the Minnesota Invasive Terrestrial Plants and Pests Center, and the USDA National Institute of Food and Agriculture, Hatch project 1006789.

**Acknowledgements:**

The authors are grateful for the Schwan Food Company Graduate Fellowship for financial support. The authors also thank Dr. Brett Arenz from the Plant Disease Clinic and Dr. Brett Barney from the Department of Bioproducts and Biosystems Engineering at the University of Minnesota – Twin Cities for reviewing parts of the manuscript and providing feedback.

**References**

1. N. Garg, F. J. Ahmad and S. Kar, *Current Research in Microbial Sciences*, 2022, **3**, 100120.
2. Y. Cao, C. Ye, C. Zhang, G. Zhang, H. Hu, Z. Zhang, H. Fang, J. Zheng and H. Liu, *Food Control*, 2022, **134**, 108694.
3. B. B. Oliveira, B. Veigas and P. V. Baptista, *Frontiers in Sensors*, 2021, **2**, 752600.
4. P. Srivastava and D. Prasad, *3 Biotech*, 2023, **13**, 200.
5. Loop-Mediated Isothermal Amplification, <https://www.neb.com/en-us/applications/dna-amplification-pcr-and-qpcr/isothermal-amplification/loop-mediated-isothermal-amplification->

- 1  
2  
3 [lamp?srsId=AfmBOooFax4qWOP2LkJQy6lbZ\\_1ioxvnG01tboxhkP7QBMMBs7g94HXS](#)).  
4 Accessed December 22,2024
- 5 6. A. M. Jankelow, H. Lee, W. Wang, T.-H. Hoang, A. Bacon, F. Sun, S. Chae, V. Kindratenko, K.  
6 Koprowski and R. A. Stavins, *Analyst*, 2022, **147**, 3838-3853.
  - 7 7. J. Liu, Z. Zeng, F. Li, B. Jiang, Y. Nie, G. Zhang, B. Pang, L. Sun and R. Hao, *Analyst*, 2024.
  - 8 8. Y. Mori, K. Nagamine, N. Tomita and T. Notomi, *Biochemical and biophysical research*  
9 *communications*, 2001, **289**, 150-154.
  - 10 9. G. Alhamid, H. Tombuloglu and E. Al-Suhaimi, *Scientific Reports*, 2023, **13**, 5066.
  - 11 10. G. Papadakis, A. K. Pantazis, N. Fikas, S. Chatziioannidou, V. Tsiakalou, K. Michaelidou, V.  
12 Pogka, M. Megariti, M. Vardaki and K. Giarentis, *Scientific reports*, 2022, **12**, 3775.
  - 13 11. X. Liu, D. Zou, C. Wang, X. Zhang, D. Pei, W. Liu and Y. Li, *Experimental and Therapeutic*  
14 *Medicine*, 2021, **21**, 1-1.
  - 15 12. Q. Fan, Z. Xie, Y. Zhang, Z. Xie, L. Xie, J. Huang, T. Zeng, S. Wang, S. Luo and M. Li, *Avian*  
16 *Pathology*, 2023, **52**, 128-136.
  - 17 13. S. Du, C. Yan, B. Du, H. Zhao, G. Xue, P. Zheng, Y. Feng, J. Cui, L. Gan and J. Feng, *Frontiers*  
18 *in Microbiology*, 2022, **12**, 816997.
  - 19 14. P. Francois, M. Tangomo, J. Hibbs, E.-J. Bonetti, C. C. Boehme, T. Notomi, M. D. Perkins and J.  
20 Schrenzel, *FEMS Immunology & Medical Microbiology*, 2011, **62**, 41-48.
  - 21 15. J.-W. Park, *Biosensors*, 2022, **12**, 857.
  - 22 16. M. Prasannakumar, P. B. Parivallal, D. Pramesh, H. Mahesh and E. Raj, *Scientific reports*, 2021,  
23 **11**, 178.
  - 24 17. M. Y. Lai, C. H. Ooi and Y. L. Lau, *Malaria journal*, 2021, **20**, 1-6.
  - 25 18. C. N. Peyrefitte, L. Boubis, D. Coudrier, M. Bouloy, M. Grandadam, H. J. Tolou and S. Plumet,  
26 *Journal of Clinical Microbiology*, 2008, **46**, 3653-3659.
  - 27 19. Y. Li, H. Xue, Y. Fei, Y. Yang, D. Huang, L. Wang, X. Xiong and X. Xiong, *Food Chemistry*,  
28 **405**, 134975.
  - 29 20. Y.-P. Zhang, J.-W. Bu, R.-X. Shu and S.-L. Liu, *Analyst*, 2024, **149**, 2507-2525.
  - 30 21. S. Wang, A. Qin, L. Y. Chau, E. W. Fok, M. Y. Choy, C. J. Brackman, G. K. Siu, C.-L. Huang,  
31 S. P. Yip and T. M. Lee, *ACS applied materials & interfaces*, 2022, **14**, 35299-35308.
  - 32 22. N. Wang, J. Gao, E. Tian, W. Yu, H. Li, J. Zhang, R. Xie and A. Chen, *Applied Microbiology and*  
33 *Biotechnology*, 2022, **106**, 1227-1239.
  - 34 23. BRET (Bioluminescence Resonance Energy Transfer) [https://www.berthold.com/en-](https://www.berthold.com/en-us/bioanalytic/knowledge/glossary/bret-bioluminescence-resonance-energy-transfer/)  
35 [us/bioanalytic/knowledge/glossary/bret-bioluminescence-resonance-energy-transfer/](https://www.berthold.com/en-us/bioanalytic/knowledge/glossary/bret-bioluminescence-resonance-energy-transfer/).  
36 Accessed August 22,2024
  - 37 24. Y. de Stigter, H. J. van der Veer, B. J. Rosier and M. Merckx, *ACS Chemical Biology*, 2024.
  - 38 25. T. Iijima, J. Sakai, D. Kanamori, S. Ando, T. Nomura, L. Tisi, P. E. Kilgore, N. Percy, H. Kohase  
39 and S. Hayakawa, *International Journal of Molecular Sciences*, 2023, **24**, 10698.
  - 40 26. T. Iijima, S. Ando, D. Kanamori, K. Kuroda, T. Nomura, L. Tisi, P. E. Kilgore, N. Percy, H.  
41 Kohase and S. Hayakawa, *PLoS One*, 2022, **17**, e0265748.
  - 42 27. R. Wu, B. Meng, M. Corredig and M. W. Griffiths, *Food and Environmental Virology*, 2023, **15**,  
43 144-157.
  - 44 28. O. A. Gandelman, V. L. Church, C. A. Moore, G. Kiddle, C. A. Carne, S. Parmar, H. Jalal, L. C.  
45 Tisi and J. A. Murray, *PloS one*, 2010, **5**, e14155.
  - 46 29. P. Hardinge, in *Bioluminescence: Methods and Protocols*, Volume 1, Springer, 2022, pp. 107-  
47 117.
  - 48 30. L. Bokelmann, O. Nickel, T. Maricic, S. Pääbo, M. Meyer, S. Borte and S. Riesenber, *Nature*  
49 *Communications*, 2021, **12**, 1467.
  - 50 31. E. Navarro, G. Serrano-Heras, M. Castaño and J. Solera, *Clinica chimica acta*, 2015, **439**, 231-  
51 250.
  - 52 32. W. Panich, S. Nak-On, M. Sabaijai, A. Raksaman, C. Puttharugsa, T. Tejangkura and T.  
53 Chontanarath, *Analytical Biochemistry*, 2024, 115481.
  - 54  
55  
56  
57  
58  
59  
60

- 1
- 2
- 3 33. S. Miyamoto, S. Sano, K. Takahashi and T. Jikihara, *Analytical biochemistry*, 2015, 473, 28-33.
- 4 34. T. N. D. Trinh and N. Y. Lee, *Lab on a Chip*, 2019, 19, 1397-1405.
- 5 35. D. A. Thai and N. Y. Lee, *Analytica Chimica Acta*, 2023, 1283, 341973.
- 6 36. Y. Wang, J. Dai, Y. Liu, J. Yang, Q. Hou, Y. Ou, Y. Ding, B. Ma, H. Chen and M. Li, *Frontiers*
- 7 *in microbiology*, 2021, 12, 609821.
- 8 37. A. Debroy, M. Yadav, R. Dhawan, S. Dey and N. George, *Folia Microbiologica*, 2022, 67, 555-
- 9 571.
- 10 38. W. Jomoui, H. Srivorakun, S. Chansai and S. Fucharoen, *Plos one*, 2022, 17, e0267832.
- 11 39. M. Li, Q. Guo, M. Liang, Q. Zhao, T. Lin, H. Gao, A. Hieno, K. Kageyama, X. Zhang and L.
- 12 Cui, *Plant Disease*, 2022, 106, 846-853.
- 13 40. G. Luo, T. Yi, Q. Wang, B. Guo, L. Fang, G. Zhang and X. Guo, *Biosensors and Bioelectronics*,
- 14 2021, 184, 113239.
- 15 41. T. N. D. Trinh and N. Y. Lee, *Journal of Biotechnology*, 2022, 357, 92-99.
- 16 42. S. Zhang, S. Lin, L. Zhu, Z. Du, J. Li, L. Wang and W. Xu, *Sensors and Actuators B: Chemical*,
- 17 2022, 372, 132544.
- 18 43. New England Biolabs, [https://www.neb.com/en-us/products/m1800-warmstart-colorimetric-](https://www.neb.com/en-us/products/m1800-warmstart-colorimetric-lamp-2x-master-mix-dna-rna)
- 19 [lamp-2x-master-mix-dna-rna](https://www.neb.com/en-us/products/m1800-warmstart-colorimetric-lamp-2x-master-mix-dna-rna)).
- 20 44. P. Rakhmat, U. Saepuloh and H. S. Darusman, *HAYATI Journal of Biosciences*, 2023, 30, 621-
- 21 631.
- 22 45. A. Çelik, A. F. Morca, O. Emiralioglu, M. Z. Yeken, G. Özer and V. Çiftçi, *Physiological and*
- 23 *Molecular Plant Pathology*, 2023, 125, 102017.
- 24 46. L.-S. Yu, S.-Y. Chou, H.-Y. Wu, Y.-C. Chen and Y.-H. Chen, *Journal of Microbiology,*
- 25 *Immunology and Infection*, 2021, 54, 963-970.
- 26 47. D. Peltzer, K. Tobler, C. Fraefel, M. Maley and C. Bachofen, *Journal of Virological Methods*,
- 27 2021, 289, 114041.
- 28 48. L. M. Diaz, B. E. Johnson and D. M. Jenkins, *Journal of biomolecular techniques: JBT*, 2021, 32,
- 29 158.
- 30 49. P. F. N. Estrela, C. A. Dos Santos, P. C. Resende, P. M. Lima, T. d. S. C. da Silva, L. Saboia-
- 31 Vahia, M. M. Siqueira, E. de Paula Silveira-Lacerda and G. R. M. Duarte, *Analyst*, 2022, 147,
- 32 5613-5622.
- 33 50. A. K. Meher, L. Aufdembrink, A. Zarouri, and A. Abbas, *The International Oak Symposium:*
- 34 *Science-based Management for Dynamic Oak Forests. Gen. Tech. Rep. SRS-278*, U.S.
- 35 Department of Agriculture, Forest Service, Southern Research Station, Asheville, NC, 2024, pp.
- 36 182–183.
- 37 51. T. A. Brown, K. S. Schaefer, A. Tsang, H. A. Yi, J. B. Grimm, A. L. Lemire, F. M. Jradi, C. Kim,
- 38 K. McGowan and K. Ritola, *Journal of biomolecular techniques: JBT*, 2021, 32, 121.
- 39 52. F. Zhang, C. Gao, L. Bai, Y. Chen, S. Liang, X. Lv, J. Sun and S. Wang, *Food Chemistry: X*,
- 40 2022, 13, 100201.
- 41 53. Y. Yu, Z. Yang, L. Wang, F. Sun, M. Lee, Y. Wen, Q. Qin and G. H. Yue, *Aquaculture and*
- 42 *Fisheries*, 2022, 7, 158-165.
- 43 54. P. Thangsunan, S. Temisak, T. Jaimalai, L. Rios-Solis and N. Suree, *Food Analytical Methods*,
- 44 2022, 1-15.
- 45 55. W. Jaroenram, I. Chatnuntawech, J. Kampeera, S. Pengpanich, P. Leaugwutiwong, B. Tondee,
- 46 S. Sirithammajak, R. Suvannakad, P. Khumwan and S. Dangtip, *Talanta*, 2022, 249, 123375.
- 47 56. S. Y. Park, D.-S. Chae, J. S. Lee, B.-K. Cho and N. Y. Lee, *Biosensors*, 2023, 13, 535.
- 48 57. S. Wu, X. Liu, S. Ye, J. Liu, W. Zheng, X. Dong and X. Yin, *Heliyon*, 2021, 7.
- 49 58. B. W. Raddatz, E. Y. S. Kim, L. M. Imamura, G. J. Steil, E. B. Santiago, S. P. T. Soares, V. H. A.
- 50 Ribeiro, B. M. M. de Almeida, S. R. Rogal Jr and M. V. M. Figueredo, *Scientific Reports*, 2022,
- 51 12, 21424.
- 52 59. C. Amaral, W. Antunes, E. Moe, A. G. Duarte, L. M. Lima, C. Santos, I. L. Gomes, G. S. Afonso,
- 53 R. Vieira and H. S. S. Teles, *Scientific Reports*, 2021, 11, 16430.
- 54
- 55
- 56
- 57
- 58
- 59
- 60

- 1  
2  
3 60. T. J. Moehling, G. Choi, L. C. Dugan, M. Salit and R. J. Meagher, *Expert Review of Molecular*  
4 *Diagnostics*, 2021, 21, 43-61.  
5 61. A. Neshani, H. Zare, H. Sadeghian, H. Safdari, B. Riahi-Zanjani and E. Aryan, *Diagnostics*,  
6 2023, 13, 155.  
7 62. M. Alsaeed, G. Alhamid, H. Tombuloglu, J. H. Kabanja, A. Karagoz, G. Tombuloglu, A. A.  
8 Rabaan, E. Al-Suhaimi and T. Unver, *Functional & Integrative Genomics*, 2024, 24, 1-12.  
9 63. A. Garrido-Maestu and M. Prado, *Comprehensive Reviews in Food Science and Food Safety*,  
10 2022, 21, 1913-1939.  
11 64. R. Logeshwari, C. Gopalakrishnan, A. Kamalakannan, J. Ramalingam and R. Saraswathi,  
12 *Frontiers in Plant Science*, 2022, 13, 1077328.  
13 65. H. Mollasalehi, F. Esmaili and D. Minai-Tehrani, *Scientific Reports*, 2023, 13, 21896.  
14 66. R. Shanker, G. Singh, A. Jyoti, P. D. Dwivedi and S. P. Singh, in *Animal biotechnology*,  
15 Elsevier, 2020, pp. 593-611.  
16 67. Y. L. Sun, C. L. Lu, C. H. Lee, E. I. Tu and C. S. Lin, *Journal of Food Safety*, 2023, 43, e13036.  
17 68. R. Sivakumar, S. Y. Park and N. Y. Lee, *ACS sensors*, 2023, 8, 1422-1430.  
18 69. T. Ruang-Areerate, C. Sukphattanaudomchoke, T. Thita, S. Leelayoova, P. Piyaraj, M. Mungthin,  
19 P. Suwannin, D. Polpanich, T. Tangchaikereee and K. Jangpatarapongsa, *Scientific reports*, 2021,  
20 11, 12152.  
21 70. C. Kong, Y. Wang, E. K. Fodjo, G.-x. Yang, F. Han and X.-s. Shen, *Microchimica Acta*, 2018,  
22 185, 1-7.  
23 71. S. Wachiralurpan, T. Sriyapai, S. Areekit, P. Sriyapai, S. Augkarawaritsawong, S. Santiwatanakul  
24 and K. Chansiri, *Frontiers in chemistry*, 2018, 6, 90.  
25 72. R. Kumvongpin, P. Jearanaikool, C. Wilailuckana, N. Sae-Ung, P. Prasongdee, S. Daduang, M.  
26 Wongsena, P. Boonsiri, W. Kiatpathomchai and S. S. Swangvaree, *Journal of virological*  
27 *methods*, 2016, 234, 90-95.  
28 73. A. N. Najian, E. E. N. Syafirah, N. Ismail, M. Mohamed and C. Y. Yean, *Analytica chimica acta*,  
29 2016, 903, 142-148.  
30 74. L. Guo, Y. Xu, A. R. Ferhan, G. Chen and D.-H. Kim, *Journal of the American Chemical*  
31 *Society*, 2013, 135, 12338-12345.  
32 75. V. T. Novi and A. Abbas, *Analytical Methods*, 2023, 15, 4640-4644.  
33 76. V. T. Novi, H. A. Aboubakr, M. J. Moore, A. Zarouri, J. Juzwik and A. Abbas, *Plant Methods*,  
34 2024, 20, 119.  
35 77. H. Wu, J.-s. He, F. Zhang, J. Ping and J. Wu, *Analytica Chimica Acta*, 2020, 1096, 130-137.  
36 78. K. Karthik, R. Rathore, P. Thomas, T. Arun, K. Viswas, K. Dhama and R. Agarwal, *MethodsX*,  
37 2014, 1, 137-143.  
38  
39  
40  
41  
42  
43  
44  
45  
46  
47  
48  
49  
50  
51  
52  
53  
54  
55  
56  
57  
58  
59  
60

1  
2  
3  
4  
5  
6  
7  
8  
9  
10  
11  
12  
13  
14  
15  
16  
17  
18  
19  
20  
21  
22  
23  
24  
25  
26  
27  
28  
29  
30  
31  
32  
33  
34  
35  
36  
37  
38  
39  
40  
41  
42  
43  
44  
45  
46  
47  
48  
49  
50  
51  
52  
53  
54  
55  
56  
57  
58  
59  
60

## **Data Availability Statement**

No primary research results, software or code have been included and no new data were generated or analyzed as part of this review.